

Effect of anisotropy on HBT radii using leptonpair interferometry

Payal Mohanty^{1,2,*}, Mahatsab Mandal^{1,†} and Pradip Roy^{1‡}

¹High Energy Nuclear and Particle Physics Division,

Saha Institute of Nuclear Physics, 1/AF Bidhannagar, Kolkata-700 064, INDIA,

²Institute of Physics and Applied Physics, Yonsei University, Seoul 120-749, Korea

(Dated: June 28, 2021)

The effect of initial state momentum-space anisotropy on invariant mass dependence of HBT radii extracted from the leptonpair interferometry is presented here. We have studied the Bose-Einstein Correlation Function (BECF) for two identical virtual photons decaying to leptonpairs at most central collision of LHC energy having fixed transverse momentum of one of the virtual photons ($k_{1T} = 2$ GeV). The *free streaming interpolating* model with fixed initial condition has been used for the evolution in anisotropic Quark Gluon Plasma (aQGP) and the relativistic (1+2)d hydrodynamics model with cylindrical symmetry and longitudinal boost invariance has been used for both isotropic Quark Gluon Plasma (iQGP) and hadronic phases. We found a significant change in the spatial and temporal dimension of the evolving system in presence of initial state momentum-space anisotropy.

PACS numbers: 25.75.+r, 25.75.-q, 12.38.Mh

I. INTRODUCTION

Two-particle intensity interferometry, commonly known as HBT interferometry is one of the efficient ways to know the space-time description of particle emission zone created in high energy nucleus-nucleus collisions [1–3]. This method was formulated and exploited by Hanbury, Brown and Twiss to measure the angular diameter of astronomical objects [4]. It was first introduced in heavy ion collision (HIC) through pion interferometry which provided valuable information about the space-time description of the system at the freeze out surface only [2]. It has been argued that in contrast to hadrons, two-particle intensity interferometry of photons and dileptons [5–12] which are produced throughout the space-time evolution of the reaction zone and which suffer almost no interactions with the surrounding medium can provide information on the the history of the evolution of the hot matter created in HIC. However photons appear to be a more restrictive probe since they are characterized only by their transverse momentum (p_T) whereas the dileptons have two kinematic variables, p_T and invariant mass(M) to play with. A soft photon (low p_T) in one frame of reference can be hard (high p_T) in another frame, whereas p_T integrated invariant mass distribution of dileptons is independent of any frame. In addition to it, p_T spectra is affected by the flow, however, p_T integrated M spectra remain unaltered by the flow in the system [13]. Also in the M spectra of dileptons, above ϕ peak, dileptons from QGP dominates

over its hadronic counterpart [14]. All these suggests that a judicious choice of p_T and M windows will be very useful to characterize the QGP and hadronic phase separately. Moreover owing to rapid longitudinal expansion at the onset of QGP phase compared to the partonic interaction rate, the anisotropy arises in $p_T - p_L$ plane with $\langle p_L^2 \rangle \ll \langle p_T^2 \rangle$ in the local rest frame. With time, such asymmetry dies out with secondary partonic interactions. After which the system is considered to be isotropic and thermal at proper time τ_{iso} and beyond $\tau \geq \tau_{iso}$ the system can be treated hydrodynamically. To include such momentum anisotropy in pre-equilibrium stage of QGP, a simple phenomenological model is adopted from refs. [15–17]. We assumed two time scales here; (i) the initial QGP formation time, τ_i , and (ii) the isotropization time, τ_{iso} , when the isotropy in momentum space is achieved and they should fulfill the criteria $\tau_i \leq \tau_{iso}$. In absence of anisotropy, we have $\tau_i = \tau_{iso}$.

In this letter, we present intensity interferometry with leptonpairs at most central LHC initial conditions at $\sqrt{s}=2.76$ TeV including momentum space anisotropy in pre-equilibrium QGP phase and attempt to study the effect of the anisotropy on the mass dependence of HBT radii extracted from the Bose Einstein Correlation Function, C_2 for two identical virtual photons which later decay into leptonpairs. We have discussed the definition and formalism of leptonpair interferometry in Sec. II, the results are given in Sec. III and finally we have summarized in Sec. IV.

II. DEFINITION AND FORMALISM

Leptonpair interferometry is based on computing the Bose-Einstein correlation (BEC) function for two

*Electronic address: payal.mohanty@gmail.com

†Electronic address: mahatsab.mandal@saha.ac.in

‡Electronic address: pradipk.roy@saha.ac.in

identical virtual photons which later decay in lepton-pairs and can be defined as [1, 11],

$$C_2(\vec{k}_1, \vec{k}_2) = \frac{P_2(\vec{k}_1, \vec{k}_2)}{P_1(\vec{k}_1)P_1(\vec{k}_2)} \quad (1)$$

where

$$P_1(\vec{k}_i) = \int d^4x \int dM_i^2 \omega(x, k_i) \quad (2)$$

and

$$P_2(\vec{k}_1, \vec{k}_2) = P_1(\vec{k}_1)P_1(\vec{k}_2) + \frac{1}{3} \int d^4x_1 d^4x_2 dM_1^2 dM_2^2 \omega(x_1, K)\omega(x_2, K) \cos(\Delta x^\mu \Delta k_\mu) \quad (3)$$

where $\vec{k}_i = (k_{iT} \cos \psi_i, k_{iT} \sin \psi_i, k_{iT} \sinh y_i)$ is the three momentum of the two identical virtual photons with $i = 1, 2$, $K = (k_1 + k_2)/2$ is the average transverse momentum, $\Delta k_\mu = k_{1\mu} - k_{2\mu} = q_\mu$, x_i and k_i are the four co-ordinates for position and momentum variables respectively and ψ_i 's are the angles made by k_{iT} with the x-axis of each virtual photon. $\omega(x, k) = dR/dM^2 d^2k_T dy$ is the source func-

tion related to the thermal emission rate of virtual photons per unit four volume. The possibility of dilution of the signal due to random pairs will not affect the HBT radii (discussed in ref [11]), thus we have neglected the leptonpairs with different invariant masses. By ignoring the leptonpair with different invarant mass, i.e, $M_1 = M_2 = M$, we can re write C_2 as:

$$C_2(\vec{k}_1, \vec{k}_2) = 1 + \frac{[\int d^4x dM^2 \omega(x, K) \cos(\Delta\alpha)]^2 + [\int d^4x dM^2 \omega(x, K) \sin(\Delta\alpha)]^2}{P_1(\vec{k}_1)P_1(\vec{k}_2)} \quad (4)$$

where $\Delta\alpha = \alpha_1 - \alpha_2$ and $\alpha_i = \tau M_{iT} \cosh(y_i - \eta) - rk_{iT} \cos(\theta - \psi_i)$, $M_{iT} = \sqrt{M^2 + k_{iT}^2}$. The inclusion of the spin of the virtual photon will reduce the value of $C_2 - 1$ by 1/3. The correlation functions can be evaluated by using Eqs. 1, 2, 3 and 4 for different average mass windows, $\langle M \rangle$. We follow Ref. [15, 16] for the dilepton production in aQGP. Beyond $\tau \geq \tau_{iso}$, the leading order process through which lepton pairs are produced in QGP is $q\bar{q} \rightarrow l^+l^-$ [18]. For low M , dilepton production from the hadronic phase the decays of the light vector mesons ρ, ω and ϕ have been considered including the continuum [19, 20]. Since the continuum part of the vector meson spectral functions are included, the processes like four pions annihilation [21] are excluded to avoid double counting.

In the present work the space time evolution is same as done in Ref. [12, 22]. For $\tau \leq \tau_{iso}$, system evolves anisotropically and is described by *free*

TABLE I: Values of the various parameters used in the evolution dynamics.

\sqrt{s}	2.76 TeV
T_i	646 MeV
τ_i	0.08 fm
T_c	175 MeV
T_{ch}	170 MeV
T_{fo}	120 MeV
EoS	2+1 Lattice QCD [23]

steaming interpolating model [15, 17]. The effect of radial flow is neglected in the anisotropic phase as it is not developed in the initial stage of the collision. For $\tau \geq \tau_{iso}$, the system is described by (1+2)d ideal hydrodynamics model with cylindrical symmetry [24] and boost invariance along the longitudinal direction [25]. The initial temperature

(T_i) and initial formation time (τ_i) of the system is constrained by the hadronic multiplicity (dN/dy) as $dN/dy \sim T_i^3 \tau_i$. The equation of state (EoS) which controls the rate of expansion/cooling has been taken from the lattice QCD calculations [23]. The chemical (T_{ch}) and kinetic (T_{fo}) freeze-out temperatures are fixed by the particle ratios and the slope of p_T spectra of hadrons [26]. The values of these parameters are displayed in Table I.

III. RESULTS

With the initial conditions described in Table I, we evaluate the correlation function, C_2 for different invariant mass windows (for $\langle M \rangle = 0.3, 0.5, 0.77, 1.02, 1.6$ and 2.5 GeV) for Pb+Pb collisions at $\sqrt{s_{NN}} = 2.76$ TeV as a function of q_{side} and q_{out} which are related to the transverse momentum of individual pair as follows: [2];

$$\begin{aligned}
 q_{side} &= \left| \vec{q}_T - q_{out} \frac{\vec{K}_T}{K_T} \right| \\
 &= \frac{2k_{1T}k_{2T} \sqrt{1 - \cos^2(\psi_1 - \psi_2)}}{\sqrt{k_{1T}^2 + k_{2T}^2 + 2k_{1T}k_{2T} \cos(\psi_1 - \psi_2)}} \\
 q_{out} &= \frac{\vec{q}_T \cdot \vec{K}_T}{|K_T|} \\
 &= \frac{(k_{1T}^2 - k_{2T}^2)}{\sqrt{k_{1T}^2 + k_{2T}^2 + 2k_{1T}k_{2T} \cos(\psi_1 - \psi_2)}} \quad (5)
 \end{aligned}$$

where k_{iT} is the individual transverse momentum and y_i is the rapidity. It may be mentioned that the BEC function has values $1 \leq C_2(k_1, k_2) \leq 2$ for a chaotic source. These bounds are from quantum statistics.

These source dimensions can be obtained by parameterizing the calculated correlation function with the empirical Gaussian form [1];

$$C_2(q, K) = 1 + \lambda \exp(-R_i^2 q_i^2) \quad (6)$$

where i stands for side and out. Thus R_{side} and R_{out} appearing in Eq. 6, are commonly referred to as HBT radii, which are measures of Gaussian widths of the source size. The deviation of λ from $1/3$ will indicate the presence of non-thermal sources. While the radius corresponding to q_{side} (R_{side}) is closely related to the transverse size of the system. The radius corresponding to q_{out} (R_{out}) measures both the transverse size and duration of particle emission [2, 3, 27–29].

In the present work, the corresponding HBT radii are extracted with the help of the parametrization expressed in Eq. 6 for three different values of τ_{iso} .

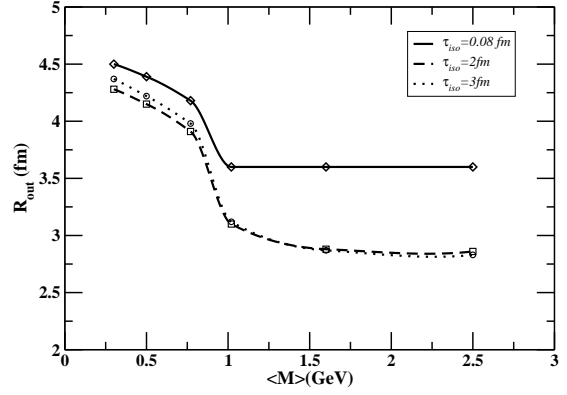


FIG. 1: The variation of R_{out} with $\langle M \rangle$ for different values of τ_{iso} . The solid line corresponds to isotropic scenario ($\tau_{iso} = \tau_i = 0.08$ fm) and the dotted and dashed line corresponds to $\tau_{iso} = 2, 3$ fm respectively which is related to anisotropic scenario.

We choose τ_{iso} in such a way that $\tau_{iso} = \tau_i$ (0.08 fm) corresponds to the isotropic situation and $\tau_{iso} > \tau_i$ (2, 3 fm) corresponds to anisotropic scenario. So basically, we have attempted to examine the sensitivity of momentum anisotropy on spatial and temporal size of the evolving system by controlling the variable, τ_{iso} . Again we argue that large M region (beyond $M \geq m_\phi$) corresponds to the partonic phase as it is dominated by lepton pairs from the partonic interactions and $M \sim m_\rho$ region corresponds to the hadronic region as leptonpairs are produced basically from the interaction of light vector mesons. So the study of invariant mass variations of R_{side} and R_{out} in these two M regions characterizes the two different phases of HIC [11]. In Figure. 1 and 2 we display the invariant mass dependence of R_{side} and R_{out} for three values of $\tau_{iso} = 0.08, 2, 3$ fm.

C_2 as function of q_{out} is calculated by taking $\psi_1 = \psi_2 = 0$, $y_1 = y_2 = 0$ and fixing transverse momentum of one photon ($k_{1T} = 2$ GeV) and varying the other (k_{2T}) for different invariant masses and the values of corresponding R_{out} is extracted from it using the parametrization given in Eq. 6. R_{out} probes both the transverse size and the duration of emission. With the development of radial flow, the transverse dimension of the emission zone decreases. Although the effect of flow is small in the initial stage of collision which is dominant in large M region (corresponds to larger size) and the duration of emission is small - resulting in a small values of R_{out} . Whereas $M \sim m_\rho$ region suffers from larger flow effects which should have resulted in a minimum value in R_{out} in this M region. However, R_{out} probes the duration of emission too, which is large for hadronic phase because of the slower expansion due to softer EoS used in the present

work for the hadronic phase. The larger duration compensates the reduction of R_{out} due to flow resulting in a bump in R_{out} for $M \sim m_\rho$ (see Fig. 1). Again by increasing τ_{iso} , the duration of particle emission shortens and results in smaller value of R_{out} .

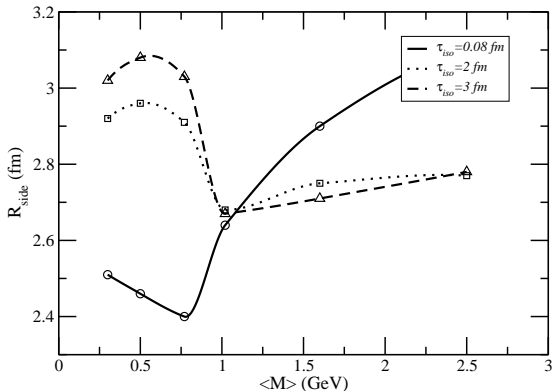


FIG. 2: The variation of R_{side} with $\langle M \rangle$ for different values of τ_{iso} . The solid line corresponds to isotropic scenario ($\tau_{iso} = \tau_i = 0.08$ fm) and the dotted and dashed line corresponds to $\tau_{iso} = 2, 3$ fm respectively which is related to anisotropic scenario.

C_2 as function of q_{side} is calculated by taking $k_{1T} = k_{2T} = 2$ GeV, $y_1 = y_2 = 0$ and fixing $\psi_2 = 0$ and varying ψ_1 for different invariant masses and the values of corresponding R_{side} is extracted from it using the parametrization given in Eq. 6. In Fig 2 we display the variation of R_{side} with M for three different values of τ_{iso} and observe quantitative as well as qualitative changes in magnitude. It can be shown that R_{side} is related to the collective motion of the system through the relation: $R_{side} \sim 1/(1 + E_{collective}/E_{thermal})$. In large M region, as the flow is not developed fully so the values of R_{side} is affected only due to initial thermal energy. As τ_{iso} is inversely related to the temperature, thus increasing τ_{iso} results in decrease in the values of R_{side} in large M region. In the mass region corresponds to the hadronic phase, $M \sim m_\rho$, the flow is fully developed and the thermal energy is reduced. The ratio of collective to thermal energy is large in this M region and hence shows smaller R_{side} in isotropic scenario. However, the situation is complex in presence of initial momentum space anisotropy. By increasing τ_{iso} , the flow is reduced resulting in larger values of R_{side} in anisotropic scenario.

The HBT radii are proportional to the average size of the system [27]. The average size of the system is related to the HBT radii (here R_{out} and R_{side})

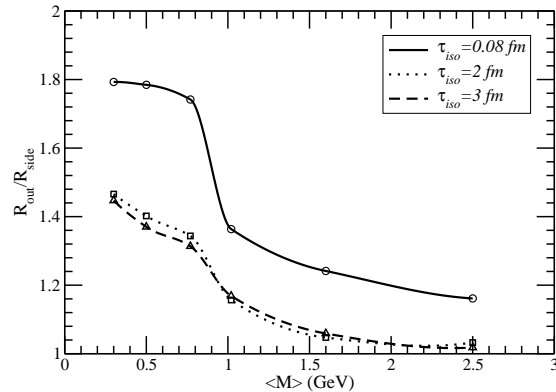


FIG. 3: The ratio R_{out}/R_{side} as a function of $\langle M \rangle$.

[27] extracted from correlation function, C_2 using Eq. 6. However, some of the model dependence gets canceled out by taking the ratio of R_{out} to R_{side} . Thus the quantity, R_{out}/R_{side} gives the duration of particle emission [1, 28, 29] for various domains of M .

Figures. 3 and 4 show the variation of R_{out}/R_{side} and $R_{diff} = \sqrt{R_{out}^2 - R_{side}^2}$ as a function of $\langle M \rangle$ for $\sqrt{s_{NN}} = 2.76$ TeV for different values of τ_{iso} . Both show a non-monotonic dependence on $\langle M \rangle$. The smaller values of both the quantities, particularly at high mass region, reflect the contributions from the early partonic phase of the system. The peak around ρ -meson mass reflects dominance of the contribution from the late hadronic phase in isotropic scenario. However, increasing values of τ_{iso} result in shorter duration of particle emission hence both these quantities have smaller value in anisotropic scenario compared to the isotropic one. However, by increasing the values of τ_{iso} we observe quantitative change in the magnitude of both of these quantities. This is because the duration of particle emission reduces as the system takes more time to become thermalized (by increasing τ_{iso}). Hence both these quantities have smaller value in the anisotropic scenario compared to the isotropic one.

IV. SUMMARY

In summary, the correlation functions for dilepton pairs have been evaluated for different values of τ_{iso} and the HBT radii have been extracted from it for Pb+Pb collision at 2.76 TeV LHC energies for different $\langle M \rangle$ windows. We observe both qualitative as well as quantitative change in the variation of HBT radii with M for dilepton pairs in presence of the initial momentum anisotropy. We argue that the variation of HBT radii with M for dilepton pairs can be used as an efficient tool to follow

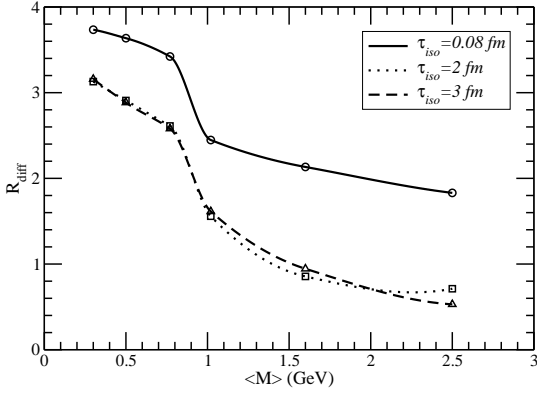


FIG. 4: The difference $\sqrt{R_{out}^2 - R_{side}^2}$ as a function of $\langle M \rangle$.

the change of the spatial and temporal dimensions

of the evolving system with time in presence of momentum space anisotropy in the initial stage of collision. The invariant mass dependence of two experimentally challenging quantities, R_{out}/R_{side} and R_{diff} also show a quantitative change due to the incorporation of anisotropy in the momentum space in the initial stage of collision. The experimental challenges for the study of dilepton interferometry is addressed in ref. [11], where it has been argued that increasing luminosity of the experiment will be a motivating factor for such measurements.

V. ACKNOWLEDGEMENTS

This work is supported by Department of Atomic Energy, India. PM is partially supported by Korean National Research Foundation.

-
- [1] S. Pratt, Phys. Rev. **D 33**, 1314 (1986).
 - [2] U. A. Weidemann and U. Heinz, Phys. Rep. **319**, 145 (1999).
 - [3] U. Heinz and B. V. Jacak, Ann. Rev. Nucl. Part. Sci. **49**, 529 (1999); T. Csörgo and B. Lörstad, Phys. Rev. C **54**, 1390 (1996); B. R. Schlei and N. Xu, Phys. Rev. C **54**, R2155 (1996); D. H. Rischke and M. Gyulassy, Nucl. Phys. A **608**, 479 (1996).
 - [4] R. Hanbury Brown and R. Q. Twiss, Nature **178**, 1046(1956).
 - [5] D. Peressounko, Phys. Rev. C **67**, 014905 (2003).
 - [6] E. Frodermann, U. Heinz, Phys. Rev. C **80** 044903 (2009).
 - [7] J. Alam, B. Mohanty, P. Roy, S. Sarkar and B. Sinha Phys. Rev. C **67**, 054902 (2003).
 - [8] S. A. Bass, B. Mueller and D. K. Srivastava, Phys. Rev. Lett. **93**, 162301 (2004).
 - [9] D. K. Srivastava and J. I. Kapusta, Phys. Lett. B **319**, 407 (1993); D. K. Srivastava, Phys. Rev. D **49**, 4523 (1994).
 - [10] D. K. Srivastava and R. Chatterjee, Phys. Rev. C **80**, 054914 (2009).
 - [11] P. Mohanty, J. Alam and B. Mohanty, Phys. Rev. C **84**, 024903 (2011); P. Mohanty, J. Alam and B. Mohanty, Nucl. Phys. A **862** 301-303, (2011). P. Mohanty, J. Alam, PoS(WPCF2011)040, (2012), arXiv : 1202.2189[Nucl-th].
 - [12] P. Mohanty, M. Mandal and P. Roy, Phys. Rev. C **89**, 054915 (2014).
 - [13] P. Mohanty, J. K. Nayak, J. Alam and S. K. Das, Phys. Rev. C **82** 034901 (2010); J. K. . Nayak and J. Alam, Phys. Rev. C **80** (2009) 064906.
 - [14] P. Mohanty, V. Roy, S. Ghosh, S. K. Das, B. Mohanty, S. Sarkar, J. e. Alam and A. K. Chaudhuri, Phys. Rev. C **85** (2012) 031903.
 - [15] M. Martinez and M. Strickland, Phys. Rev. Lett. **100**, 102301 (2008).
 - [16] M. Martinez and M. Strickland, Phys. Rev. C **78**, 034917 (2008).
 - [17] B. Schenke and M. Strickland Phys. Rev. D **76**, 025023 (2007).
 - [18] J. Cleymans, J. Fingberg and K. Redlich, Phys. Rev. D **35**, 2153 (1987).
 - [19] J. Alam, S. Raha and B. Sinha, Phys. Rep. **273**, 243 (1996); J. Alam, S. Sarkar, P. Roy, T. Hatsuda and B. Sinha, Ann. Phys. **286**, 159 (2001); R. Rapp and J. Wambach, Adv. Nucl. Phys. **25**, 1 (2000).
 - [20] E. V. Shuryak, Rev. Mod. Phys. **65**, 1 (1993).
 - [21] P. Lichard and J. Juran, Phys. Rev. D **76**, 094030 (2007).
 - [22] L. Bhattacharya and P. Roy, Phys. Rev. C **78**, 064904 (2008), L. Bhattacharya and P. Roy, Phys. Rev. C **79**, 054910 (2009).
 - [23] C. Bernard *et al.*, Phys. Rev. D **75** 094505 (2007).
 - [24] H. von Gersdorff, M. Kataja, L. McLerran and P. V. Ruuskanen, Phys. Rev. D **34**, 794 (1986).
 - [25] J. D. Bjorken, Phys. Rev. D **27**, 140 (1983).
 - [26] T. Hirano and K. Tsuda, Phys. Rev. C **66**, 054905 (2002).
 - [27] D. H. Rischke and M. Gyulassy, Nucl. Phys. A **608**, 479 (1996).
 - [28] M. Herrmann and G. F. Bertsch, Phys. Rev. C **51**, 328 (1995).
 - [29] S. Chappman, P. Scotto and U. Heinz, Phys. Rev. Lett. **74**, 4400 (1995).